Chapter 4

Fullerene Dynamics with X-Ray Free-Electron Lasers

Nora Berrah

Additional information is available at the end of the chapter

http://dx.doi.org/10.5772/intechopen.70769

Abstract

Ultrafast and ultra-intense, short X-ray pulses from free-electron lasers (FELs) have opened up a new regime for all scientific research and for fullerenes in particular. FELs allow for the investigation of ultrafast nonlinear and multiphoton processes, as well as the exploration of the fragmentation dynamics of fullerenes. This chapter describes the FELs' attributes that enable new FEL-based investigations. In particular, we report on the X-ray ionization and fragmentation of C_{60} under high- and mid-fluence femtosecond pulses, from the Linac Coherent Light Source (LCLS), at SLAC National Accelerator Laboratory. We also describe the X-ray ionization and fragmentation with low-fluence X-ray pulses of the endohedral fullerene ($Ho_3N@C_{80}$). We end our contribution by presenting opportunities for future time-resolved dynamics research using pump-probe techniques.

Keywords: fullerenes, photoionization, fragmentation, ions, photons, free-electron laser, FEL, LCLS, femtosecond, attosecond, X-rays, dynamics, pump probe, C_{60}, $Ho_3N@C_{80}$

1. Introduction

Fullerenes, which bridge the gap between molecules and nanoparticles, are ideal systems for investigating the dynamical behavior of extended systems when exposed to X-rays. Fullerenes and their derivatives, characterized by their hollow geometric structures and nanometer-sized outer diameter, draw a great deal of interest due to their wide range of applications and "supramolecular" physical and chemical properties [1]. Fullerenes have displayed molecular [2] and bulk [3] behavior and have proven to be an excellent testing ground for experiments and theories [4].

This chapter, which is not a review, focuses on the interaction of intense lasers with fullerenes—and in particular, with X-ray free-electron lasers (FELs). After brief, general introductions on the interaction of fullerenes with strong laser fields using tabletop lasers and on

endohedral fullerenes, ultrafast and ultra-intense free-electron lasers (FELs) are described; we focus our report on the interaction of C_{60} and of the endohedral $Ho_3N@C_{80}$ fullerene with a specific FEL: the Linac Coherent Light Source (LCLS) at SLAC National Accelerator Laboratory.

In recent years, the nonlinear physics research in atoms, molecules, and clusters that were conducted using strong laser fields has led to various phenomena, such as the generation of attosecond pulses [5]. The behavior of molecules in short, intense laser fields [6] was extended to large molecules, such as C_{60}, which is intriguing due to the numerous nuclei-electron responses exhibited, because it is a cage of 60 atoms with 240 valence-electrons [7–16]. The interaction of such a large system is key to investigating many-body problems induced on the system's electrons by the photon electric field. The photon interaction with the electronic fullerene's degrees of freedom results in electronic dynamics that lead to nuclei dynamics, because they are both interconnected. Fullerenes, including endohedral fullerenes, are ideal candidates to explore their many-body responses to electromagnetic fields because they respond in different ways—depending upon the field parameters [7–17]. Ionization, which is one of the possible reactions, has shown to occur on different time scales.

The laser photoionization mechanisms of fullerenes have been found to be wavelength and pulse duration-dependent [9, 10, 18]. For IR pulses (800 nm) of about 30 fs duration and intensities below 5×10^{13} W/cm^2, it was found that multiphoton processes dominate when ionizing C_{60}, while tunneling, and/or over-the-barrier ionization and ionization due to induced electron re-collision [8] have a low probability to occur under these conditions. The single-active-electron (SAE) method was used to calculate the ionization of C_{60} in intense, 4×10^{13} W/cm^2 laser pulses with durations between 27 and 70 fs, and for a wide range of wavelengths ranging from 395 to 1800 nm [19]. This calculation agreed with measurements by Shchatsinin et al. [12]. For a long IR wavelength of 1800 nm and 70 fs pulse duration, the SAE picture predicts "over the barrier" ionization for a peak intensity of 10^{15} W/cm^2, leading to non-fragmented but highly charged C_{60}^{q+} (q = 1–12) [7]. At a short wavelength of 355 nm, the excitation of C_{60} with 10 ns pulses leads to fragmentation by delayed ionization and C_2 emission, as well as other fragments—even for small intensities of about 2×10^6 W/cm^2 [15]. The use of electron spectroscopy in addition to the ion measurements allowed new questions to be posed, such as the impact of multi-electron dynamics and whether the ionization and the fragmentation dynamics be adequately modeled in the SAE picture [12]. This latter work resulted in other recent experimental and theoretical investigations, which concluded that both SAE and many-electron effects are important [8].

Trimetallic nitride template (TNT) endohedral metallofullerenes (EMFs), which consist of a trimetallic nitride moiety and a fullerene host, have also sparked broad interest in many fields—including materials chemistry, organic chemistry, biomedicine, biomedical chemistry, and molecular device design [20–23]. In addition to the fundamental photodynamics interest, EMFs carry the expectation or hope to act as radiotherapy agents to treat tumors while significantly reducing the X-ray dose for patients. Functional groups can be attached to the endohedral fullerene shell to bind the molecules to a specific site in order to deliver toxic, high-Z metal atoms, which are enclosed inside [24, 25]. Endohedral fullerenes have high stability, which is an inherent advantage for resisting biologically induced cage-opening [26].

This is thought to help protect healthy tissues from the toxic metals. Monochromatic X-rays could be used to resonantly excite the high-Z atom, restricting the X-ray radiation damage to the cells that need to be treated, while leaving surrounding tissues largely unaffected by the radiation dose. In our case, we are interested in exploring the X-ray absorption and response of EMF with ultrashort X-rays.

2. FELs as tools for fullerene dynamics

A new class of intense and short-wavelength lasers, the FELs [27–32], has opened up new research opportunities for many scientific fields, from physics to chemistry, as well as matter under extreme conditions and biology. These vuv/X-ray lasers are accelerator-based tools, which are hybrid, as far as their attributes are concerned, between synchrotron facilities and typical tabletop lasers. FEL typically employs linear accelerators to drive relativistic electron beams through long undulators, characterized by alternating magnetic field, in order to produce intense radiation [32, 33]. **Figure 1** shows a schematic of the LCLS FEL undulator [34]. This type of insertion device, which was key for high-brightness third-generation synchrotron light sources, enable, if they are long enough, the production of ultra-intense vuv/X-ray radiation with femtosecond (fs) pulse duration [27, 30–32].

The use of FELs is unique despite the availability of fs and attosecond tabletop lasers to investigate ultrafast fullerenes and cluster dynamics. FELs add new attributes to tabletop lasers because they provide very high fluence (>10^{18} photon/pulse) in a wide, tunable photon energy range (10 eV–12 keV) that is not yet achievable with any tabletop laser. One of the essential attributes of the use of short wavelengths is to enable element selectivity, which permits selecting a specific atom in any system. Furthermore, short wavelengths allow for site selectivity, which

Figure 1. Schematic of the 33 m long LCLS FEL undulator [34].

thus targets a specific atomic shell in any system. This provides atomic-scale spatial resolution, which is very important for delineating the effects of each atom in a given system. Because FELs target atomic orbitals instead of molecular orbitals, they allow simple measurements of the response of inner-shell electrons (localized with each atom composing the molecule), compared to the complex response of the molecular orbitals composed of all valence electrons. Probing inner-shell electrons with short wavelengths allows efficient probing of physical and chemical phenomena in fullerenes or clusters from within, in an inside-out ionization.

Tabletop laser technology is also progressing to shorten the wavelength and increase the pulse energy, in order to enable study of photon-matter interactions as well—by ionizing or scattering from inner-shell electrons. Short-wavelength FELs also provide femtosecond pulse duration to study nuclear dynamics. Tabletop laser technology has already progressed to provide attosecond pulses, thus allowing the probing of electronic properties of given systems. In parallel, FEL scientists are also working hard at shortening their photon pulses; for example, the LCLS is aiming to produce ~600–400 attoseconds X-ray pulses in the fall of 2017. This new development will allow time-resolved studies of not only nuclear [5] but electronic molecular dynamics as well [35]. These new FEL-based xuv or X-ray photon sources initiate the photodynamics by core ionization. The initial charge is induced with high degrees of temporal and spatial localization, thus making the data analysis easier to handle. The new FEL family of ultrafast xuv/X-ray complement and extend the work carried out by tabletop lasers [36], xuv [37], synchrotron [38], or photon sources.

FELs are emerging photon tools that have been available since 2005, with the first vuv FLASH FEL at DESY in Germany [31] becoming available to scientists. The first X-ray FEL, the LCLS, was commissioned and available to scientists while being commissioned in 2009 [27, 30]. One of the most important attributes of FELs is their tunability within a wide frequency range. They currently span a photon energy range of about 10 eV to 12 keV, with pulse energies that exceed 3 mJ. This includes a repetition (rep) rate of up to 120 Hz, including a fs time scale where the pulse duration can be as short as 2–3fs and as long as 500 fs. The LCLS FEL aims to provide ~600–400 attoseconds in the soft X-ray regime by December 2017, which is an unprecedented progress. This new breakthrough will push the frontiers of science and may result in new science.

In addition to the X-ray LCLS FEL in the United States [27, 30] and the hard X-ray SACLA FEL in Japan's Riken laboratory [28], there are four vuv FEL counterparts: FLASH-1 and FLASH-2 at DESY [31], Germany; SCSS in Spring-8 Japan [28]; and FERMI in Trieste, Italy [29]. Other FELs that will be available this year, in 2017, are as follows: the large European XFEL project at DESY, Germany, will be available in the fall of 2017; a hard and soft X-ray FEL in South Korea called PAL-XFEL; and the SwissFEL at the Paul Scherrer Institute in Switzerland. Other FELS are either amidst planning in Sweden or in construction for the soft-X ray LCLS-II FEL in the United States.

Most FELs produce their photons via the self-amplified spontaneous emission (SASE) process, which is a stochastic process; thus, FEL laser pulses build up from noise and consist of a number of randomly spaced spikes of 1–5 fs duration within an energy envelope of about 15 eV—if it is not monochromatized—giving rise to *not* well-defined laser pulse profiles. The only exception so far is the FERMI FEL, which is a laser-seeded FEL that has similar pulse profiles compared to tabletop lasers. In addition, the FERMI FEL [29] produces a high-pulse energy,

20–100 μJ, between 14 and 62 eV, with ~100 fs pulse duration, and the spectral width is typically $\Delta\lambda/\lambda \approx 1 \times 10^{-3}$ (FWHM). The combination of these parameters surpasses tabletop lasers. Progress toward the X-ray FEL pulse shape is happening; however, the LCLS has introduced a so-called self-seeding, where a tunable element—typically a crystal or grating monochromator—is inserted halfway through the undulators to filter a specific wavelength for further amplification. This provides higher stability and reduces the laser bandwidth from 20 to 0.5 eV (e.g., 0.75 eV bandwidth at 8450 eV photon energy). The XFEL, in Hamburg, Germany, which will be operating in the fall of 2017, will utilize a new technology based on superconducting linacs, in order to accelerate the electrons that produce the FEL photon pulses, with higher brightness and a higher repetition (rep) rate. This high rep rate of ~1 MHz enables highly differential measurements, such as e-ion-ion coincidence techniques that can delineate dynamics. These coincidence techniques will allow the examination of both electronic and nuclear dynamics, in real time, subsequent to photo-absorption, which is important for ultrafast chemistry.

If one were to compare tabletop lasers and FELs, he or she would state that they are complementary light sources, with their own advantages and challenges. The drawback with the tabletop lasers is the need to overcome their low-pulse intensity in the xuv-X-ray regime, as well as their short-range frequency tunability. They can provide weak intensity attosecond pulses, thus enabling electronic dynamics research in some cases [36]. Tabletop lasers deliver higher rep rates (~100 kHz) compared to FELs (120 Hz). However, as stated above, the XFEL in Germany will offer MHz rep rates in 2017. FELs, like synchrotron light sources, interact with inner-shell electrons instead of molecular orbitals. In fact, all FELs produce high-pulse intensity in the X-ray regime, which is ten orders of magnitude higher compared to synchrotron radiation. The broad tunability, with the use of monochromators, enables the exploration of resonance structures and enables wavelength-dependent experiments.

All short-wavelength light sources enable inner-shell ionization, which is followed by the Auger decay—thus, the absorption of one photon leads to the emission of two electrons, as shown in **Figure 2**. With ultra-intense FELs, the fluence is so high that multiple absorptions of photons occur, leading to sequential multiphoton ionization.

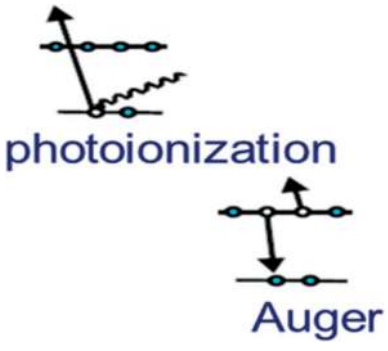

Figure 2. Schematic of the photoionization and Auger decay mechanism.

3. Ionization and fragmentation dynamics of C_{60} with the LCLS and FEL

The ionization and fragmentation of C_{60} were investigated experimentally and theoretically by using intense, fs, X-ray FEL pulses. The goal was to understand the response of a relatively large, strongly bonded molecule and to quantitatively understand the fs dynamical effects initiated by intense X-ray exposure. This is important to fundamental nonlinear physics research progress in general. It also directly impacts both the study of matter under extreme conditions and the area of biomolecular imaging. Imaging viruses and proteins, at an atomic spatial scale and on the time scale of atomic motion, requires quantitative understanding—which is best accomplished through spectroscopic measurements of a system that is simpler than a biomolecule—instead of scattering experiments. In other words, studying fullerenes, this is the first step toward understanding in a large system how a multiply ionized fullerene leads to slow electrons, which in turn initiate radiation damage in biological systems [39]. Therefore, the photoionization of C_{60} with intense FEL pulse is relevant to imaging of biomolecules, because such a study revealed the influence of processes that were not known or reported prior to our work [40].

The structure determination of biomolecules is done by imaging these systems using X-ray scattering experiments. These studies need photon brightness to obtain the images, which unfortunately induces electronic and structural radiation damage—thus altering the sample despite the use of short pulse durations [41]. Calculations have shown that high-intensity X-ray pulses trigger a cascade of damage processes in ferredoxin crystals, which are a metalloprotein of particular interest to the biology community [41, 42]. Furthermore, intense X-ray FEL pulses were found to modify the electronic properties of C_{60} on a fs time scale, based on observations of the diffraction of intense 32-fs X-ray pulses by a powder sample of crystalline C_{60} [41]. These radiation damages need to be evaluated, and spectroscopic measurements can reveal information that is not available with scattering experiments.

C_{60} was chosen as a benchmark molecule because of its chemically bonded carbon atoms, whose bond lengths and damage processes can emulate biomolecules. The fs experimental and theoretical C_{60} investigation dynamics was studied in the gas phase, with intense 485 eV photon energy to take advantage of the large photo-absorption cross section of carbon 1s electrons. We aimed to reach conditions in which approximately each C atom within a C_{60} molecule in the focus of X-ray pulse absorbs multiple photons during the X-ray pulse duration.

The experiment was carried out at the AMO hutch at the LCLS. The fullerenes (C_{60} and $Ho_3N@C_{80}$) were introduced into the vacuum through a heated oven source. For the C_{60} experiment, a 2m-long-magnetic-bottle time-of-flight spectrometer [43] was used to measure the ions and electrons that resulted from the ionization [40]. The spectrometer is shown in **Figure 3**, while a zoom of the interaction region is displayed in **Figure 4**; the oven appears as a cylinder from the top, the spectrometer's permanent magnet sticks to the left of the figure, and the spectrometer lens is shown to the right side of **Figure 4**.

We chose three pulse durations 4, 30, and 90 fs to explore the effect of the X-ray pulse duration on the C_{60} ionization. As explained with **Figure 2**, the inner-shell ionization will lead to

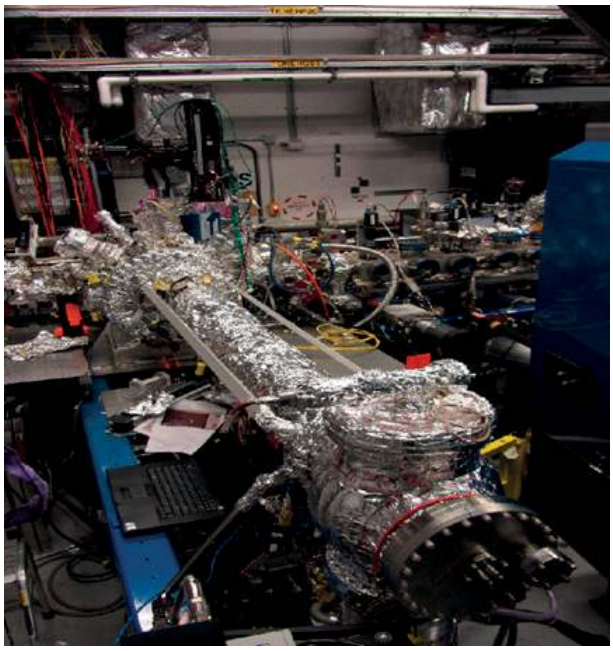

Figure 3. Picture of the AMO hutch installation. The 2m-long-magnetic-bottle spectrometer, wrapped in aluminum foil, is shown sticking out from the interaction chamber.

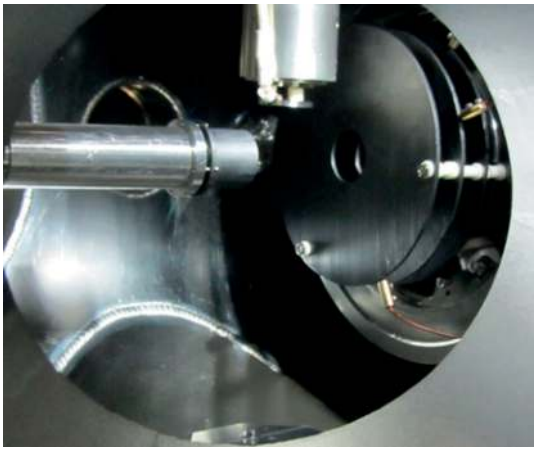

Figure 4. Close-up view of the interaction region showing the nozzle part of the oven, the permanent magnet, and the spectrometer lens (see details in the text).

the Auger process, but with a high-fluence X-ray FEL pulse, this results in many photo- and Auger electrons due to the cyclic, multiphoton ionization until the pulse duration is over. Additionally, this photoionization process leads to secondary ionization of C_{60}, as well as of its

fragment ions by the photo- and Auger electrons. The C_{60} molecule charges up to C_{60}^{8+} based on our data. The X-ray pulse is not homogeneous, as described in Section 2. Therefore, depending upon where C_{60} lands in the X-ray pulse, it can fragment in different scenarios. If C_{60} lands outside of the focus of the X-ray FEL pulse, it will fragment, as shown in **Figure 5**, into molecular ion strands with either a ring or linear structure. **Figure 5** shows the mass-to-charge ratio (M/Q), displaying the parent C_{60} ionized up to q = 8+ along with the molecular ions C_m^+, m = 1–11.

If C_{60} lands in the focus of the FEL pulse, because of the short C—C bond lengths, it fragments via the Coulomb repulsion into small molecular carbon ions and atomic carbon charge-state distribution from C^+ to C^{6+}. Therefore, C can be fully stripped with 90 fs pulse duration [40] as shown in **Figure 6**. In this case, the pulse is intense and long enough for the C atom to undergo at least three cyclic photoionization-Auger decays, leading to C^{6+}.

As shown in **Figure 6**, the charge-state distribution depends upon the pulse duration. At the shorter pulse duration we used (4fs), the highest charge state obtained is C^{5+} indicating that at least two cyclic photoionization-Auger decays occurred [40, 44]. Our measurements (light color data) were compared with calculation (dark color data) in order to understand the different physical and chemical effects, giving rise to the observed charge-state distribution.

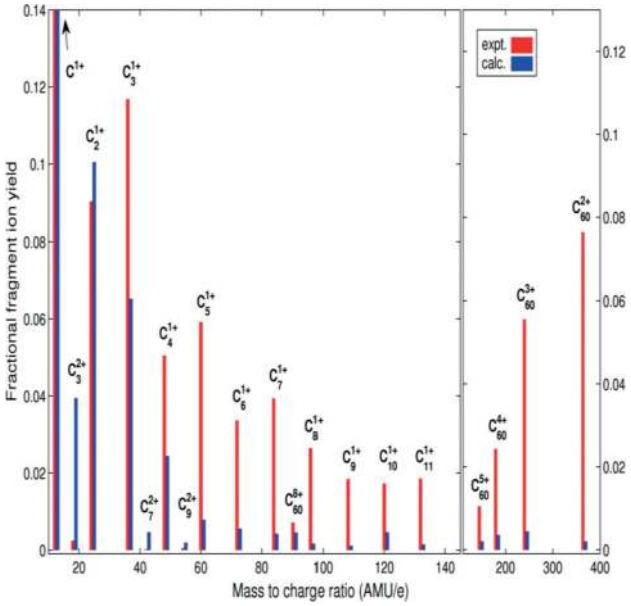

Figure 5. Time-of-flight spectrum showing the fragmentation of C_{60} with mid-fluence LCLS X-ray pulses. Light color data are experiment while dark color data are theory.

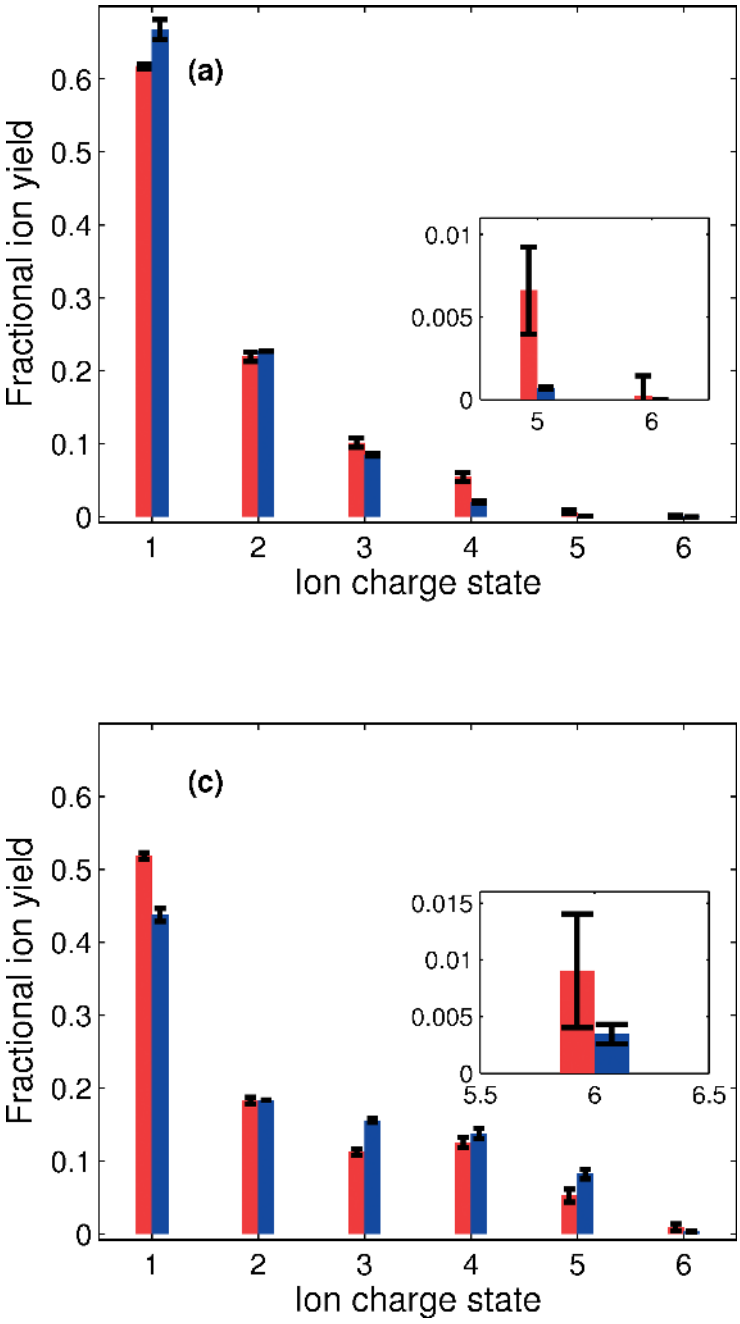

Figure 6. Atomic carbon charge-state distribution resulting from the Coulomb explosion of C_{60} under high-fluence X-ray FEL pulses. (a) corresponds to data taken with 4f pulse duration while (c) corresponds to data taken with 90 fs pulse duration.

3.1. Discussion

With current computer technology, it is not possible to carry out ab initio calculations via quantum mechanical methods. The best that can be done is to develop classical physics models that describe the dynamics of atoms/ions and electrons that appear in the continuum after photoionization. These models include, for example, the rate equations of the ionization and the C ionization cross sections that are directly resulting from quantum mechanical calculations [45, 46]. The model used in this FEL-based C_{60} work consists of a mixed molecular dynamics (MD) Monte Carlo tool based on treating C atoms [47]. The real-space dynamics of atoms, ions, and the (quasi-) free electrons resulting from photoionization and Auger decay is described by Newtonian mechanics. In this methodology, C_{60} is modeled as 60 individual carbon atoms. The atoms' electronic configuration is tracked and changed stochastically during each time step (0.8 attosecond) by using a Monte Carlo scheme. During the many ionization events, new electrons that are released from their bound atomic orbitals are treated classically, with the appropriate energies, as they "appear" in the system. The C atoms were held together by a fullerene-specific classical Brenner force field, and the charges interacted via Coulomb forces. In order to mimic a molecule, the model needed to contain several physical and chemical processes that were revealed through the experiment. **Figure 6** shows a good agreement between the model and the experiment, but in the initial comparison, they did not agree. The model originally predicted more abundant C ion charge states, which revealed that there was *strong recombination* between the released electrons from photoionization and the ions after the FEL pulse ends.

The comparison between the model and the experimental data not only led to the interpretation of our experiment but also led to solid improvement in the MD calculation. Specifically, the model had to include several physical and chemical processes: (1) bond-breaking in C_{60} was modeled by setting the bonding force field to zero between two C-charged ions; (2) the secondary ionizations arising from free electrons colliding with and ionizing atoms/ions was included; (3) the molecular Auger effect consisted of sharing the energy and using two carbon atoms in the release of the two electrons. This was taken into account by removing the ejected electron from the L-shell of a neighboring C atom, while the 1s vacancy of an ion was filled up with its own L-shell electron; and (4) the recombination of a classically trapped electron if it were no longer delocalized among several C ions but instead localized to only one C ion.

Figure 7 shows the effect of the MD modeling, where we compare the data and the model for two pulse durations, 30 and 90 fs. As can be seen, there is no effect with the two different pulse durations, which thus revealed that the dynamics might already be over with the use of a 30 fs X-ray pulse. This means that the physical and chemical processes included might have occurred within 30 fs.

In order to explain the comparison between the model and the data, we display in **Figure 7** the C ion yield *difference* between the model and the experiment on the Y-axis. The smallest value of the bars corresponds to the best agreement between the model and the experiment. Each yield corresponds to the sum of the charge-state distribution (C^{1+}–C^{6+}) shown in **Figure 7**. The X-axis displays bars that correspond to the several different physical and chemical processes, which were included in the model. As described above, each of these processes were included

http://dx.doi.org/10.5772/intechopen.70769

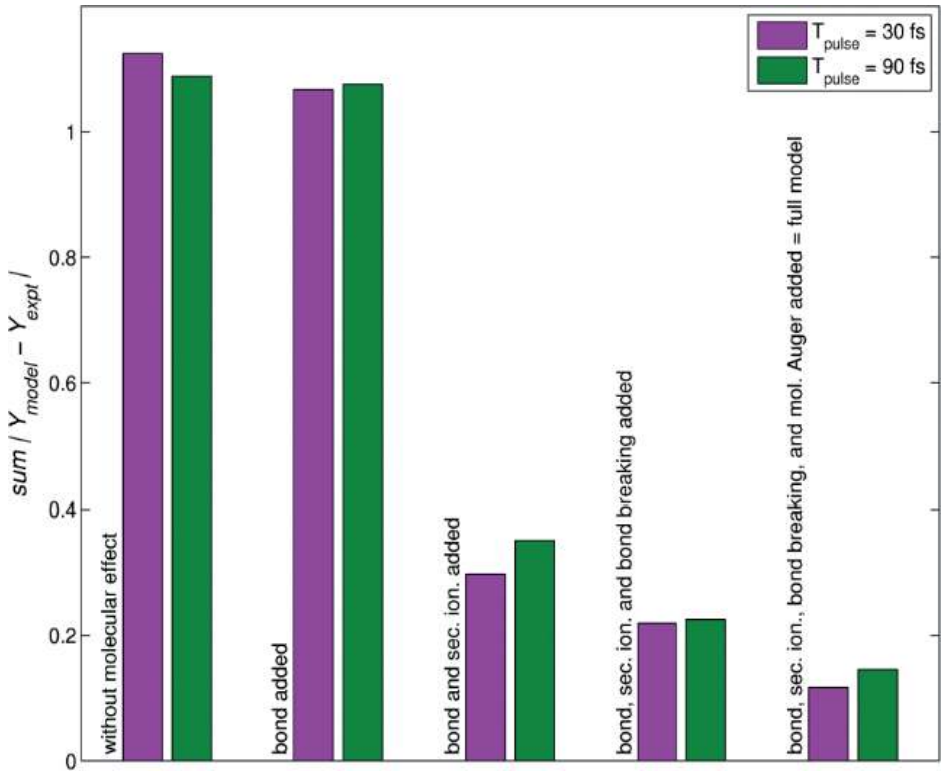

Figure 7. Comparison between the experimental data and the model (see text for details).

one at a time to display their importance. As can be seen, molecular effects and molecular bonds slightly contributed to a better agreement. The dramatic effect is obtained in the case of the secondary ionization of C_{60} by the photo- and Auger-electrons. This effect is weak in small, isolated molecules and van der Waals clusters; it is completely absent in atoms. As can be seen, the addition of molecular bond-breaking and molecular Auger improved even more the model.

This combined theoretical and experimental work illustrates the successful use of *classical mechanics* to describe all moving particles in C_{60}. The work clearly revealed the influence of processes not previously suspected or reported. The impact we aimed to achieve was also realized because this fullerene spectroscopic work quantitatively demonstrated electronic damage due to photoelectron and Auger electrons interacting with the ions as a secondary ionization effect. Our results were corroborated with recent separate calculations [39]. Finally, one of the goals of the MD model was to build a new approach that would scale with larger systems, such as biomolecules. This work demonstrated that the modeling [40, 44] coached by experiment was successful and can be applicable for X-ray interactions with any extended system—even at higher X-ray dose rates that are expected with future FEL sources, such as the soon-to-be available XFEL in Germany and with the future LCLS-II.

4. Ionization and fragmentation dynamics of $Ho_3N@C_{80}$

The C_{60} work described above led us to consider exploring increased complexity by choosing the interaction of endohedral fullerenes (also called doped fullerenes) with FELs. These systems are even more intriguing than C_{60}, because they host a moiety that ranges from an atom to a molecule. Nothing was known about their structure or dynamics when excited with X-ray FEL. As mentioned in the introduction, these nanoscale systems have received attention in part because they can be used for applications ranging from medical usage [48] to drug delivery, as well as their possible use for quantum computing [49]. Our interest, however, stems from exploring a fundamental point of view, the fragmentation of $Ho_3N@C_{80}$ induced by short, X-ray pulses from the LCLS FEL.

The experiment was carried out at the AMO hutch using a time-of-flight spectrometer [50] for detecting the ions produced in the interaction of the endohedral fullerenes with the LCLS pulses. The experiment on $Ho_3N@C_{80}$ was carried out with 1530 eV in order to selectively target the ionization from a specific shell, which was the Ho 3d. The pulse duration of the X-ray pulse was 80 fs with a pulse energy of about 6.7×10^{15} photons/cm^2. This experiment had less fluence than the experiment on C_{60} by two orders of magnitude due to a different transport of the photon beam through the optics [50]. We estimate that the fluence used in the $Ho_3N@C_{80}$ is only ¼ of the fluence used in C_{60} [40], thus resulting in only a few multiphoton ionization cycles. **Figure 8** shows three time-of-flight spectra that result from the multiphoton ionization processes of $Ho_3N@C_{80}$ with intense X-ray FEL. We show in **Figure 8** three panels that focus on the singly, doubly, and triply ionized parent.

The top panel, which spans the mass-to-charge ratio (M/Q) from 350 to 1300, depicts structures attributed to multiply charged fullerenes' parent ions from singly charged $Ho_3N@C_{80}^+$ to quintuply charged $Ho_3N@C_{80}^{5+}$ (albeit weak). This clearly shows that the fluence for this experiment is weaker than for the C_{60} experiment we described above since in **Figure 5** the parent ions were charged up to C_{60}^{8+}. It is also clear that the atomic Ho^+ ion has the highest yield compared to all other ion fragments. This must arise from the fragmentation of the encapsulated Ho_3N moiety—thus, indicating that the three multiply charged Ho atoms, which were selected to be the most ionized compared to N or C atoms, freed themselves from the C_{80} cage. The middle panel focuses on the doubly and triply ionized parent molecule along with doubly ionized fullerene molecules that lost C dimers such as $Ho_3N@C_{78}^{2+}$, $Ho_3N@C_{70}^{2+}$, and $Ho_3N@C_{50}^{2+}$. The loss of C dimers was also observed previously with tabletop experiments [2]; however, the shrunk cage size to C_{50} was never previously observed. The bottom panel shows the triply and quadruply charged parent fullerenes, along with triply ionized parent fullerenes that lost C dimers, namely, $Ho_3N@C_{78}^{3+}$, $Ho_3N@C_{76}^{3+}$, $Ho_3N@C_{70}^{3+}$, and $Ho_3N@C_{50}^{3+}$.

Figure 9 shows other fragments that occur in the 160–240 M/Q range. The prominent signal is the atomic Ho^+ ion which escaped the cage. Other fragment ions are C molecular ion chains or rings such as C_{15}^+ and C_{17}^+ along with surprising new fragments such as HoC_2^+, $HoCN^+$, HoC_4^+, and HoC_3N^+ [51].

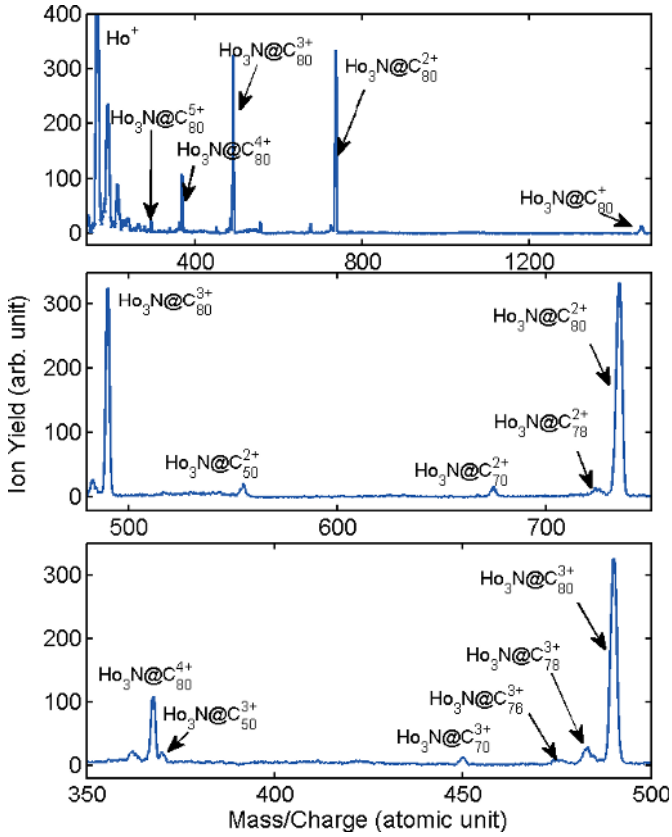

Figure 8. Ion yield M/Q spectra shown in three panels. The top panel depicts a wide M/Q fragment ions, while the middle and bottom fragments focus on doubly and triply charged parent ions (see text for details).

4.1. Discussion

This experiment was carried out in the low-fluence regime, since we estimated that about eight photons were absorbed by $Ho_3N@C_{80}$. In the C_{60} experiment, described in Section 3, we appraised that about 180 photons were absorbed per C_{60} molecule. The photoionization with 1530 eV leads to the absorption cross section of Ho to be about 1.55 Mb, while that of C was about 0.013 Mb. Our interpretation of the interaction of $Ho_3N@C_{80}$ with 1530 eV photon energy was that the Ho atom charges up and gets multi-ionized due to the cyclic photoionization and Auger decay [51]. In doing so, it grabs electrons from the carbon cage via electron transfer between the Ho and the cage—resulting in the whole parent molecule charging up and reaching at least $Ho_3N@C_{80}^{5+}$, as observed in **Figure 8**. We assumed that as the carbon cage charges up, it would become unstable and will break apart, thus leading to molecular

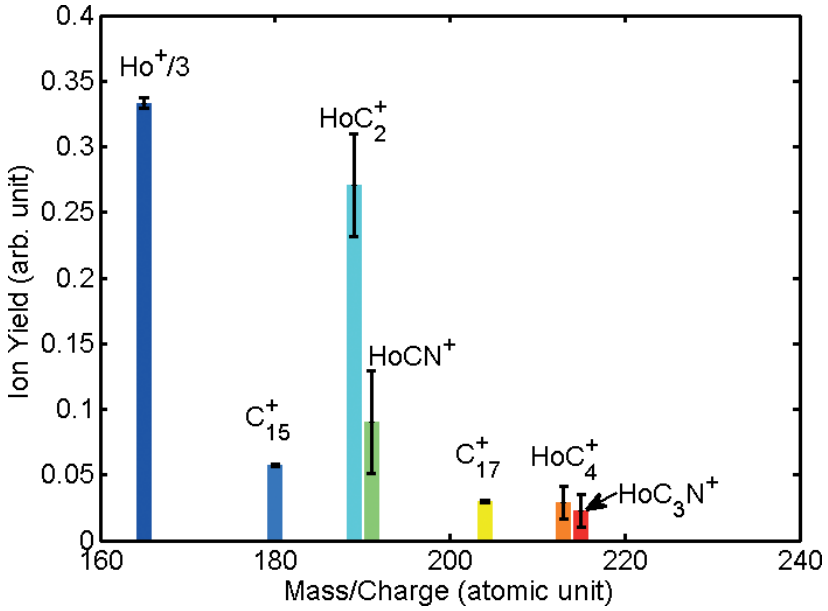

Figure 9. Ion spectrum displaying M/Q focusing on Ho ion and the Ho-based molecular fragments ion (see text for details).

fragment ions. The Ho atoms are about ten times heavier than the C atoms, and, therefore, we assume that they will not move faster than the carbon cage. We clearly have evidence of bond-breaking and bond-forming since we observed in **Figure 9** the following fragments: HoC_2^+, $HoCN^+$, HoC_4^+, and HoC_3N^+. It is unclear if the moiety first breaks into three Ho atoms and the N atoms and then the carbon cage fragments or if the reverse occurs. It is also unclear how the new bonds have formed. This is to be determined by future time-resolved experiments that might track the ionization and fragmentation dynamics and decipher the mechanisms leading to the final ionic states we observed. Additionally, we hope that our work will stimulate the development of molecular dynamics simulations suitable for endohedral fullerenes and for even larger molecules exposed to intense XFEL.

5. Measuring time-resolved dynamics using pump-probe techniques with FELs

Pump-probe spectroscopy techniques, championed by tabletop lasers [36], allow the measurement of dynamics for any system—from atoms to fullerenes and from solids to biological specimens. They are being used extensively, and the ultimate goal is to determine the motions and locations of nuclei and electrons and to determine the energy flow and charge transfer in systems. Recording these motions and making "molecular movies" using pump-probe spectroscopy seem reachable in the near future due to the new technologies.

Pump-probe techniques with FELs offer similar opportunities to measure physical and chemical changes in molecules at an atomic spatial resolution (on the time scale of atomic motion). With attosecond, the goal is to also measure the electronic motion. These techniques can be used for the study of fullerenes, in order to tackle fundamental questions such as, *how do the atoms in the fullerenes move after the photon energy is deposited in the fullerenes?* How do the bonds between the atoms that make the fullerenes break, or what are the pathways for the induced atomic motion in fullerenes? These questions can be asked and answered with FELs using pump-probe techniques. As in standard pump-probe work, to capture the dynamics, the pump pulse initiates the motions, and a probe pulse detects the changes using as many time delays as needed between the pump and probe pulses, ideally in a wide time scale. In order to achieve this goal, one needs two pulses, which can be generated in a few ways: (1) the accelerator scientists have developed several methods, but the most recent one cuts fresh slices from the electron bunch. They manipulate the electron bunch before it enters a split undulator, so that only its tail is lasing, in order to produce the first X-ray pulse. Next, they delay the electron bunch in order to acquire a time delay and spoil the electron bunch orbit further, by having the head of the bunch lasing and thus using a fresh slice from the electron bunch to produce the second photon pulse [52]. This scheme is also capable of providing two X-ray colors [52]; (2) the FEL pulse can be split into two X-ray pulses with an X-ray split and delay tool [53]. These two schemes were used successfully in experiments in the mode of X-ray pump-X-ray probe; and (3) a third scheme utilizes an X-ray pulse from the FEL as either the pump or the probe, and it is paired with a short tabletop pulse laser [54] (IR or UV). All of these schemes have been used in various FELs.

The FEL-based experiments, paired most of the time with pump-probe techniques, are carried out by using various types of spectrometers or imaging detectors for absorption experiments or for diffractive scattering experiments, respectively. The latter holds the promise to achieve imaging of molecules in the gas phase. Double VMI spectrometers paired with X-ray/IR, for a pump-probe scheme, are also used to measure the electrons—as well as the ions using the ion-ion coincidence techniques. These differential techniques examine both electronic and nuclear dynamics following the interaction of fullerenes with FEL X-ray pulses and also resolve the transient electronic rearrangement that accompanies photoionization [55]. The current repetition (rep) rate for the operational FEL facilities is at most 120 Hz (lower than the current tabletop repetition rate of 1–100 KHz), which does not allow easy FEL-based electron-ion-ion coincidence studies—although some work has been done in this highly differential mode [56]. However, the new XFEL in Hamburg, Germany, which will be completed by the end of this year, will offer ~1 MHz rep rate—thus allowing the measurement of e-ion-ion coincidences to track and precisely determine the decay channels and time it takes for the ultrafast nuclear dynamics to occur. It seems that the dream of making molecular movies is reachable in the next few years.

6. Conclusions

The investigation of the ionization and fragmentation of fullerenes with FELs is at its infancy. This work reported on the first two spectroscopic experiments on C_{60} and $Ho_3N@C_{80}$ using ion

spectroscopy but much more needs to be accomplished. These first experiments need to be followed by time-resolved studies to delineate the nuclear dynamics, including electron transfer, using e-ion-ion coincidence techniques or using diffraction techniques and imaging. In addition, the next generation of attosecond FELs will allow the exploration and hopefully understanding of electron migration between atoms using photoelectron spectroscopy. Finally, the work done on C_{60} was conclusive because of the close interaction with theories and modeling. We hope that the reported work will stimulate theorists to tackle the many-body interactions resulting from the interaction of fullerenes with femtosecond or attosecond X-ray or vuv FELs.

Acknowledgements

We thank all of the authors of references [40, 44, 51]. We also thank Ms. Rachel Tshonas for her help with the manuscript. This work was funded by the Department of Energy, Office of Science, Basic Energy Sciences (BES), Division of Chemical Sciences, Geosciences, and Biosciences under grant no. DE-SC0012376.

Author details

Nora Berrah

Address all correspondence to: nora.berrah@uconn.edu

Physics Department, University of Connecticut, Storrs, CT, USA

References

[1] Supramolecular Chemistry of Fullerenes and Carbon Nanotubes. In: Martin N, Nierengarten JF, editors. Wiley-VCH Verlag GmbH & Co. KGaA; 2012. DOI: 10.1002/9783527650125

[2] Johansson JO, Campbell EEB. Probing excited electronic states and ionisation mechanisms of fullerenes. Chemical Society Reviews. 2013;**42**:5661-5671. DOI: 10.1039/C3CS60047E and references therein

[3] Feng M, Zha J, Petek H. Atomlike, hollow-core-bound molecular orbitals of C_{60}. Science. 2008;**320**:359-362 and references therein. DOI: 10.1126/science.1155866

[4] Mignolet B, Johansson JO, Campbell EEB. Probing rapidly ionizing super-atom molecular orbitals in C_{60}: A computational and femtosecond photoelectron spectroscopy study. Chemphyschem. 2013;**14**:3332-3340. DOI: 10.1002/cphc.201300585 and references therein

[5] Krausz F, Stockman MI. Attosecond metrology: from electron capture to future signal processing. Nature Photonics. 2014;**8**:205-213. DOI: 10.1038/nphoton and references therein

[6] Zhao SF, Le AT, Jin C, Wang X, Lin CD. Analytical model for calibrating laser intensity in strong-field-ionization experiments. Physical Review A. 2016;**93**:023413. DOI: 10.1103/PhysRevA.93.023413

[7] Bhardwaj VR, Corkum PB, Rayner DM. Internal laser-induced dipole force at work in C_{60} molecule. Physical Review Letters. 2003;**91**:203004 and references therein. DOI: 10.1103/PhysRevLett.91.203004

[8] Huismans Y, et al. Macro-atom versus many-electron effects in ultrafast ionization of C_{60}. Physical Review A. 2013;**88**:013201. DOI: 10.1103/PhysRevA.88.013201

[9] Campbell EE, et al. From above threshold ionization to statistical electron emission: The laser pulse-duration dependence of C_{60} photoelectron spectra. Physical Review Letters. 2000;**84**:2128

[10] Kjellberg M, et al. Momentum-map-imaging photoelectron spectroscopy of fullerenes with femtosecond laser pulses. Physical Review A. 2010;**81**:023202. DOI: 10.1103/PhysRevA.81.061602

[11] Bohl E, et al. Relative photoionization cross sections of super-atom molecular orbitals (SAMOs) in C_{60}. The Journal of Physical Chemistry A. 2015;**119**:11504-11508. DOI: 10.1021/jp408147f

[12] Shchatsinin I, et al. C_{60} in intense short pulse laser fields down to 9 fs: excitation on time scales below e-e and e-phonon coupling. The Journal of Chemical Physics. 2006; **125**:194320. DOI: http://dx.doi.org/10.1063/1.2362817

[13] Campbell EEB, Hoffmann K, Rottke H, Hertel IV. Sequential ionization of C_{60} with femtosecond laser pulses. The Journal of Chemical Physics. 2001;**114**:1716. DOI: http://dx.doi.org/10.1063/1.1584671

[14] Tchaplyguine MHK et al. Ionization and fragmentation of C_{60} with sub-50 fs laser pulses. The Journal of Chemical Physics. 2000;**112**:2781. DOI: http://dx.doi.org/10.1063/1.480852

[15] Lebeault MA, et al. Decay of C_{60} by delayed ionization and C_2 emission: Experiment and statistical modeling of kinetic energy release. The Journal of Chemical Physics. 2012;**137**:054312. DOI: http://dx.doi.org/10.1063/1.4737926

[16] Li H, et al. Coherent electronic wave packet motion in C_{60} controlled by the waveform and polarization of few-cycle laser fields. Physical Review Letters. 2015;**114**:123004. DOI: 10.1103/PhysRevLett.114.123004

[17] Xiong H, Mignolet B, Fang L, Osipov T, Thomas T, Wolf JA, Sistrunk E, Gühr M, Remacle R, Berrah N. The role of super-atom molecular orbitals in doped fullerenes in a femtosecond intense laser field. Scientific Reports. 2017;**7**:121

[18] Li H, et al. Transition from SAMO to Rydberg state ionization in C_{60} in femtosecond laser fields. The Journal of Physical Chemistry Letters. 2016;**7**:4677-4682. DOI: 10.1021/acs.jpca.5b11713

[19] Jaroń-Becker A, Becker A, Faisal FHM. Single-active-electron ionization of C_{60} in intense laser pulses to high charge states. The Journal of Chemical Physics. 2007;**126**:124310. DOI: 10.1021/acs.jpca.5b11713

[20] Fatouros PP et al. In vitro and in vivo imaging studies of a new endohedral metallofullerene nanoparticle. Radiology. 2006;**240**:756. DOI: 10.1148/radiol. 2403051341

[21] Fillmore HL, et al. Conjugation of functionalized gadolinium metallofullerenes with IL-13 peptides for targeting and imaging glial tumors. Nanomedicine. 2011;**6**:449-458. DOI: 10.2217/nnm.10.134

[22] Popov AA, Yang S, Dunsch L. Endohedral fullerenes. Chemical Reviews. 2013;**113**:5989-6113. DOI: 10.1021/cr300297r

[23] Zhang J, Stevenson S, Dorn HC. Trimetallic nitride template endohedral metallofullerenes: Discovery, structural characterization, reactivity, and applications. Accounts of Chemical Research. 2013;**46**:1548. DOI: 10.1021/ar300301v

[24] Cagle DW, Kennel SJ, Mirzadeh S, Alford JM, Wilson LJ. In vivo studies of fullerene-based materials using endohedral metallofullerene radiotracers. Proceedings of the National Academy of Sciences of the United States of America. 1999;**96**:5182-5187

[25] Meng J, Liang X, Chen X, Zhao Y. Biological characterizations of $[Gd@C_{82}(OH)_{22}]_n$ nanoparticles as fullerene derivatives for cancer therapy. Integrative Biology. 2013;**5**:43. DOI: 10.1039/C2IB20145C

[26] Stevenson S et al. Small-bandgap endohedral metallofullerenes in high yield and purity. Nature. 1999;**401**:55. DOI: 10.1038/43415

[27] Emma P, et al. First lasing and operation of an ångstrom-wavelength free-electron laser. Nature Photonics. 2010;**4**:641-647. DOI: 10.1038/nphoton.2010.176

[28] Ishikawa T, Allaria E, et al. Ultrafast X-ray pulse characterization at free-electron lasers. Nature Photonics. 2012;**6**:540-544. DOI: 10.1038/nphoton.2012.276

[29] Allaria E, et al. Two-stage seeded soft-X-ray free-electron laser. Nature Photonics. 2012;**6**:699-704. DOI: 10.1038/nphoton.2013.277

[30] Berrah N, Bucksbaum PH. The Ultimate X-ray Machine. Scientific American. 2014;**310**:64-71. DOI: 10.1038/scientificamerican0114-64

[31] Ackermann W et al. Operation of a free-electron laser from the extreme ultraviolet to the water window. Nature Photonics. 2007;**1**:336-342. DOI: 10.1038/nphoton.2007.76

[32] Bucksbaum P, Berrah N. Brighter and faster: The promise and challenge of the X-ray free-electron laser. Physics Today. 2015;**68**:25-32. DOI: 10.1063/PT.3.2845

[33] Berrah N, Bucksbaum PH. The ultimate X-ray machine. Scientific American Special Collector's Edition. 2015;**54**:7

[34] Figure 1 from SLAC site: https://portal.slac.stanford.edu/sites/lcls_public/Pages/Default.aspx

[35] Kraus PM, et al. Measurement and laser control of attosecond charge migration in ionized iodoacetylene. Science. 2015;**350**:790-795. DOI: 10.1126/science.aab2160

[36] Leone SR, McCurdy CW, Burgdoerfer J, Cederbaum LS, Chang Z, Dudovich N, Feist J, Greene CH, Ivanov M, Kienberger R, Keller U, Kling MF, Loh ZH, Pfeifer T, Pfeiffer AN, Santra R, Schafer K, Stolow A, Thumm U, Vrakking MJJ. Charge migration in molecules. Nature Photonics. 2014;**8**:162-166. DOI: 10.1038/nphoton.2014.48

[37] Calegari F, et al. Ultrafast electron dynamics in phenylalanine initiated by attosecond pulses. Science. 2014;**346**:336-339. DOI: 10.1126/science.1254061

[38] Sann H, Havermeier T, et al. Imaging the temporal evolution of molecular orbitals during ultrafast dissociation. Physical Review Letters. 2016;**117**:243002. DOI: 10.1103/PhysRevLett.117.243002

[39] Stumpf V, Gokhberg K, Cederbaum LS. The role of metal ions in X-ray-induced photochemistry. Nature Chemistry. 2016;**8**:237-224. DOI: 10.1038/nchem.2429

[40] Murphy BF, et al. Femtosecond X-ray-induced explosion of C_{60} at extreme intensity. Nature Communications. 2014;**5**:4281. 1-9 and references therein. DOI: 10.1038/ncomms5281

[41] Abbey B, et al. X-ray laser–induced electron dynamics observed by femtosecond diffraction from nanocrystals of Buckminsterfullerene. Science Advances. 2016;**2**:1-5 and references therein. DOI: 10.1126/sciadv.1601186

[42] Nass K, et al. Indications of radiation damage in ferredoxin microcrystals using high-intensity X-FEL beams. Journal of Synchrotron Radiation 2015;**22**(1):1-14. ISSN: 1600-5775 and references therein. DOI: 10.1107/S1600577515002349

[43] Eland J, Vieuxmaire O, Kinugawa T, Lablanquie P, Hall R, Penent F. Complete two-electron spectra in double photoionization: The rare gases Ar, Kr, and Xe. Physical Review Letters. 2003;**90**:053003. DOI: 10.1103/PhysRevLett.90.053003

[44] Berrah N, Fang L, Osipov T, Jurek Z, Murphy BF, Santra R. Emerging photon technologies for probing ultrafast molecular dynamics. Faraday Discussions. 2014;**171**(1):471-485. DOI: 10.1039/C4FD00015C

[45] Son SK, Santra R. Investigating dynamics of complex system irradiated by intense X-ray free electron laser pulses. Journal of Phys. Conf. Series; 2011 XATOM—an integrated toolkit for X-ray and atomic physics (CFEL, DESY)

[46] Son SK, Young L, Santra R. Impact of hollow-atom formation on coherent X-ray scattering at high intensity. Physical Review A. 2011;**83**:033402-033413. DOI: 10.1103/PhysRevA.83.033402

[47] Jurek Z, Faigel G, Tegze M. Dynamics in a cluster under the influence of intense femtosecond hard X-ray pulses. European Physical Journal D: Atomic, Molecular, Optical and Plasma Physics. 2004;**29**:217-229. DOI: 10.1140/epjd/e2004-00033-3

[48] Melanko JB, Pearce M, Salem A. Nanotubes/nanorods/nanofibers/fullerenes for nanoscale drug delivery. Nanotechnology in Drug Delivery; Springer Science/American Association for Pharmaceutical Scientists (AAPS). 2007;105-127

[49] Harneit W, et al. Room Temperature electrical detection of spin coherence in C_{60}. Physical Review Letters. 2007;**98**:216601. DOI: 10.1103/PhysRevLett.100.199904

[50] Hoener M, Fang L, Kornilov O, Gessner O, Pratt S, Guehr M, Kanter E, Blaga C, Bostedt C, Bozek J, et al. Ultraintense X-ray induced ionization, dissociation, and frustrated absorption in molecular nitrogen. Physical Review Letters. 2010;**104**:253002. DOI: 10.1103/PhysRevLett.104.253002

[51] Berrah N, Murphy B, Xiong H, Fang L, Osipov T, Kukk E, Guehr M, Feifel R, Petrovic VS, Ferguson KR, Bozek JD, Bostedt C, Frasinski LJ, Bucksbaum PH, Castagna JC. Femtosecond X-ray induced fragmentation of fullerenes. Journal of Modern Optics. 2015;**3**(4):390-401. DOI: 10.1080/09500340.2015.1064175

[52] Lutman I, Maxwell T, MacArthur J, Guetg M, Berrah N, Coffee R, Ding Y, Huang MZA, Moeller S, Zemella J. Fresh-slice multicolour X-ray free-electron lasers. Nature Photonics. 2016;**10**:745. DOI: 10.1038/nphoton.2016.201

[53] Berrah N, Fang L, Murphy B, Kukk E, Osipov T, Coffee R, Ferguson K, Xiong H, Castagna JC, Petrovic V, Montero S, Bozek J. A two mirrors X-ray pulse split and delay instrument for femtosecond time resolved investigations at the LCLS free electron laser facility. Optics Express. 2016;**24**(11):11768-11781. DOI: 10.1364/OE.24.011768

[54] McFarland B, Farrell J, Miyabe S, Tarantelli F, Aguilar A, Berrah N, Bostedt C, Bozek J, Bucksbaum P, Castagna J, et al. Ultrafast X-ray Auger probing of photoexcited molecular dynamics. Nature Communications. 2014;**5**:4235. DOI: 10.1038/ncomms5235. DOI:10.1038/ncomms5235

[55] Erk B, et al. Imaging charge transfer in iodomethane upon X-ray photoabsorption. Science. 2014;**345**:288-291 and references therein. DOI: 10.1126/science.1253607

[56] Moshammer SK, Jaeschke E, et al. Synchrotron light sources and free-electron lasers. Springer International Publishing Switzerland. 2016;1291-1322. DOI: 10.1007/978-3-319-14394-1-26